Current Optics and Photonics
Vol. 2, No. 5, October 2018, pp. 443-447

ISSN: 2508-7266(Print) / ISSN: 2508-7274(Online)
DOI: https://doi.org/10.3807/COPP.2018.2.5.443

Optimization of Diode-pumped Cesium Vapor Laser Using Frequency Locked Pump Laser

Seongjin Hong, Byungjoo Kong, Yong Soo Lee, and Kyunghwan Oh*

Institute of Physics and Applied Physics, Yonsei University, Seoul 03722, Korea

(Received July 12, 2018 : revised August 6, 2018 : accepted August 6, 2018)

We propose a diode-pumped cesium laser using frequency locking of a pump laser that can effectively increase the maximum output power of the cesium laser. We simultaneously monitored the absorption spectrum of cesium and the laser output power, and the frequency of pump laser was locked at the center of the D_2 absorption line of the cesium atom to obtain an effective gain enhancement. Using this scheme, we have achieved output power increase of ~0.1 W compared to when frequency locking was not applied. Furthermore, by optimizing the temperature of the cesium cell and the reflectivity of the output coupler, we successfully achieved an output power of 1.4 W using the pump power of 2.9 W, providing a slope efficiency of 61.5% and optical-to-optical efficiency of 49%.

Keywords : Cesium vapor laser, Diode-pumped alkali laser, Frequency locking, Atomic vapor
OCIS codes : (140.0140) Lasers and laser optics; (140.1340) Atomic gas lasers; (140.3480) Lasers, diode-pumped; (140.3425) Laser stabilization

I. INTRODUCTION

The diode-pumped alkali laser (DPAL) has been extensively researched as one of the most promising candidates for high power and efficiency lasers [1-3]. The most important advantages of DPALs are high quantum efficiency 95.3% for cesium (Cs), 98.1% for rubidium (Rb), and 99.6% for potassium (K), an excellent beam quality, reduced thermal problems as a gaseous gain medium, and narrow linewidth [4, 5]. Furthermore, the stimulated cross section, which was collisionally broadened by ethane buffer gas, is several orders larger than the cross section of a common solid-state laser [6-8]. Thus, all these properties and features show that DPAL is being regarded as a promising alternative to the scalable high power laser system [9-11].

Unlike other types of lasers, in DPAL the linewidth of the D_2 absorption line of the alkali atom is extremely narrow for optical pumping with full width half maximum (FWHM) less than a few hundreds of MHz, which could be broadened to be ~10 GHz allowed by buffer gas [4, 5, 8]. The broadened linewidth is still narrow for optical pumping compared to commercial laser diodes (LD), and an overlap between the bandwidth of LD and the linewidth of D_2 absorption would severely affect the optical-to-optical efficiency, slope efficiency, and output laser power in the DPAL [12, 13]. For this reason, the short-term frequency stability of the pump laser is not adequate for the DPAL without active stabilization of the pump laser frequency [14, 15]. Therefore, active controlling and stabilizing the frequency of the pump laser can directly serve a benefit in output and stability increase of the DPAL [16].

In this study, we experimentally achieved a continuous-wave Cs vapor laser using frequency locking of the pump laser. We simultaneously monitored the absorption spectra of cesium and the laser output power with scanning of pump frequency around the D_2 line of Cs, and the frequency of the pump laser was fixed at the maximum absorption frequency to result in an effective gain enhancement. Using this scheme, an output power increase of ~0.1 W could be obtained with an output power of 1.4 W, an optical-to-optical efficiency of 49%, and a slope efficiency of 61.5%. Furthermore, in order to optimize the

*Corresponding author: koh@yonsei.ac.kr, ORCID 0000-0003-2544-0216

Color versions of one or more of the figures in this paper are available online.

laser efficiency, we varied the reflectivity of output coupler and temperature of the Cs cell in the laser cavity. To the best of knowledge of the authors, this paper is the first time for DAPL operation with a frequency locked pump laser. We believe that this proposed method could be further applied to a scalable high power DPAL.

II. EXPERIMENTS

Figure 1 shows the energy diagram of Cs lasers, which is composed of the ground level $^6S_{1/2}$, the first excited level $^6P_{1/2}$, and the second excited level $^6P_{3/2}$ [4, 5]. As shown in Fig. 1, two resonance transitions of $^6P_{1/2} \rightarrow {}^6S_{1/2}$ and $^6P_{2/3} \rightarrow {}^6S_{1/2}$ are called the D_1 transition and the D_2 transition, respectively [4, 5]. The transition wavelength of D_1 and D_2 and the quantum efficiency are listed in Table 1. The linewidth of the D_2 transition could be collisionally broadened to achieve spectrally homogeneous transition by an ethane buffer gas [8]. In this study, the D_2 absorption line of the Cs atom was broadened by 500 Torr ethane buffer gas. The pump LD operating at ~852 nm excited the atoms to the $^6P_{3/2}$ state, which is rapidly relaxed to the upper laser level $^6P_{1/2}$ state by collision with ethane buffer gas. This could create a population inversion and lasing at 894 nm [4, 5].

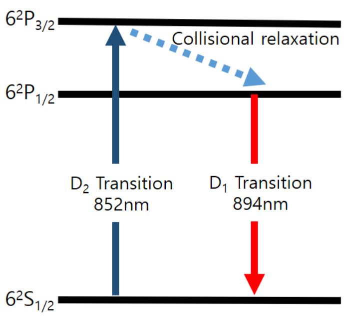

FIG. 1. The three-level energy diagram of Cs atom, which is composed of the ground level $^6S_{2/1}$, the first excited level $^6P_{3/2}$, and the second excited level $^6P_{1/2}$. The laser is pumped on the D_2 transition at 852 nm, and emitted on the D_1 transition at 894 nm.

TABLE 1. Atomic parameters of Cs vapor laser

Parameters	Value
λ_{D2} (nm)	852.35
λ_{D1} (nm)	894.95
Quantum efficiency	95.2%

The experimental set-up is schematically shown in Fig. 2. In order to simultaneously monitor the absorption of the pump laser and the laser output, two equivalent Cs cells are employed in the pump absorption measurement set-up and the laser cavity set-up. The pump laser was split into two optical paths by a beam splitter, 0.5% of it was used for frequency locking of the pump laser and 99.5% of it was used for the laser. The wavelength tunable Littrow-type external cavity diode laser (ECDL) was used as the single frequency pump source [17-19]. This pump laser could provide wavelength scanning whose mode-hop-free tuning range is 15 GHz with repetition rate of 10 Hz [17-19]. It produces about 2.9 W continuous wave power at 852 nm with a linewidth ~10 kHz.

The right column of Fig. 2. shows the laser cavity structure. The L-shape 20-cm-long laser cavity consisted of a concave high reflecting mirror with a curvature radius of 25 cm whose reflectivity is higher than 99.5% at both $\lambda =$ 852 nm and 894 nm and a flat output coupler. Optical paths to the pump and the laser beams were separated by a polarization beam splitter (PBS). The 2 cm long sealed cell with Cs vapor and 500 Torr of ethane buffer gas was used as an optical gain medium. The silica cell had circular

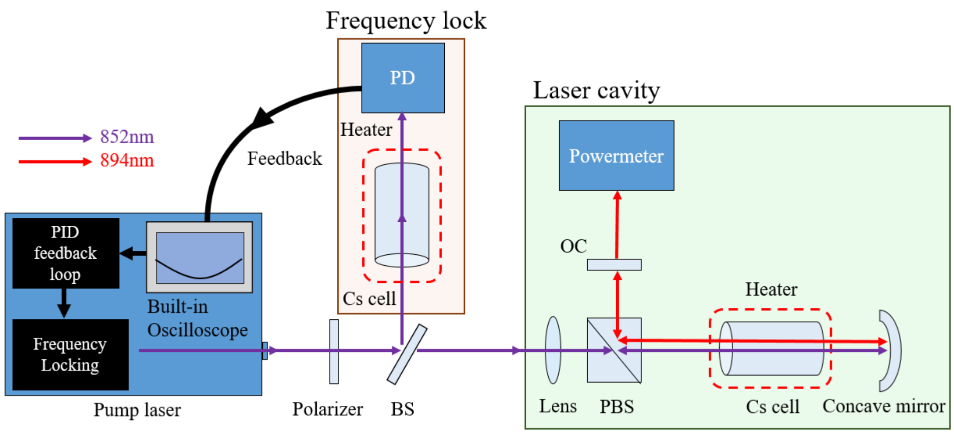

FIG. 2. Schematic diagram of the proposed DPAL set-up to simultaneously monitor the absorption of pump laser and the laser output for the frequency locking. The pump absorption measurement set-up and the laser cavity are in parallel. The frequency locking of the pump by a separate Cs vapor cell on the left and the lasing experiment on the right were executed simultaneously (BS: Beam splitter, PBS: Polarization beam splitter, OC: Output coupler, PID: proportional-integral-derivative).

windows of 2.5 cm diameter, which were anti-reflection coated on both sides for securing a high transmission at the pump wavelength $\lambda = 852$ nm and laser output $\lambda = 894$ nm. The temperature of the Cs cell was controlled by heater. In order to optimize the laser output, we varied the reflectivity of output coupler and the temperature of the Cs vapor cell.

The frequency locking set up is schematically shown in the center column of Fig. 2. 0.5% of the pump laser power passes through a Cs vapor cell equivalent to that in the laser cavity set-up. The pump laser through the frequency lock Cs cell could be detected by photo detector (PD), which is connected to a built-in oscilloscope in the pump laser driver. By scanning the frequency of the pump laser around the absorption lines of Cs, the absorption spectrum could be obtained, and proportional-integral-derivative (PID) feedback loop locks the frequency of the pump laser near to the maximum absorption wavelength [20-22].

In Fig. 3(a), there are transmission spectra of both pure Cs (red line) without buffer gas and Cs with 500 Torr ethane buffer gas (black line). In this figure, we could clearly see the two absorption peaks of pure Cs due to hyperfine energy level of ground state $^6S_{1/2}$ F = 3 and F = 4 [23, 24], and broadened absorption peak by buffer gas, whose overall absorption range was not measured due to the limitation of mode-hop-free range (15 GHz) in our pump laser. As shown in Fig. 3(b), the frequency of the pump laser was locked at near the absorption peak to maximize the output power of the laser. Using this frequency locking scheme, we could obtain a power increase of ~0.1 W compared to output power when frequency locking was not applied. Detailed gain dynamics needs to be further investigated in our laser scheme, which is being pursued by the authors.

The reflectivity of the output coupler and the temperature of the Cs vapor mainly have significant influence on the output performance [25-28]. In order to obtain the maximum output of the laser, we experimentally optimized

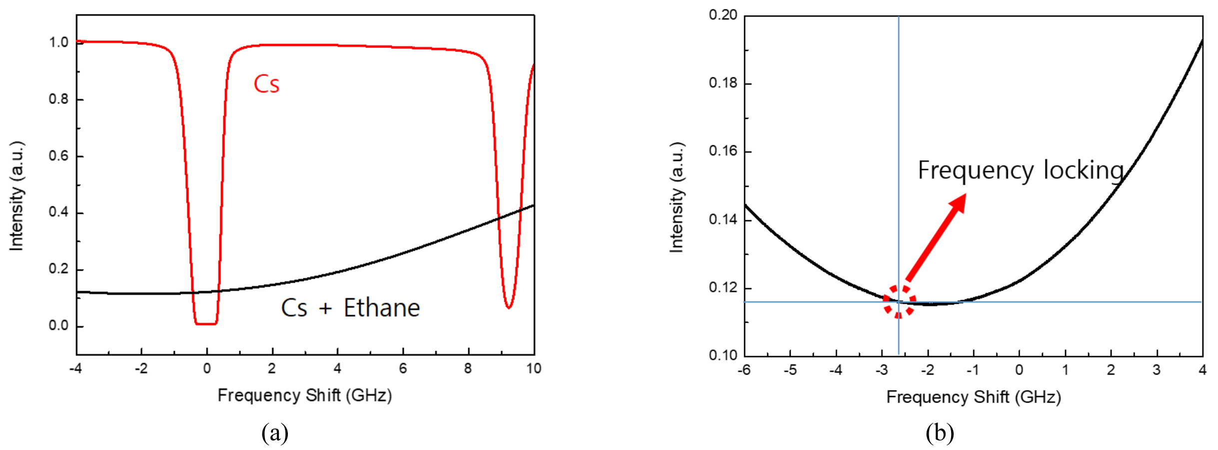

FIG. 3. (a) The absorption spectra of pure Cs vapor without buffer gas (red line) and Cs vapor with 500 Torr ethane buffer gas (black line). (b) The frequency locking point near the center of the absorption peak with Cs vapor with 500 Torr ethane. Using this frequency locking, the output power could be increased ~0.1 W.

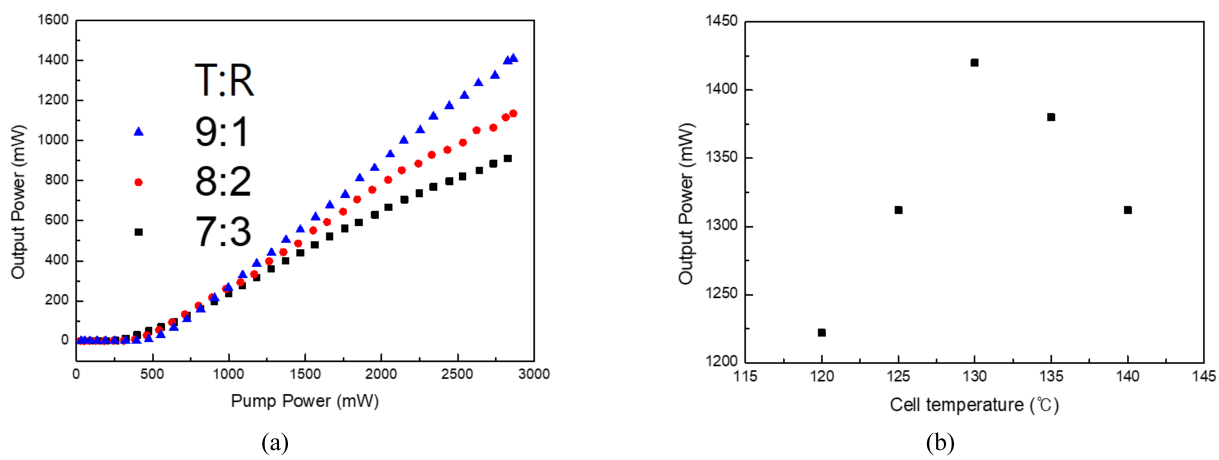

FIG. 4. The output laser power (a) versus the pump power with 10%, 20%, 30% of output coupler reflectivity and (b) versus temperature from 120 to 140°C. The optimized output coupler reflectivity is 10% and temperature is 130°C.

the reflectivity of output coupler and temperature of the Cs cell. The experimental dependence of laser output power on the pump power was measured for the output couplers with reflectivity 30, 20, and 10% in Fig. 4(a). The corresponding measured values of the output power for these output couplers are 0.91, 1.1, and 1.4 W, and the slope efficiency are 38.2, 48, and 61.5%, respectively with 2.9 W of pump power at 130°C. Fei *et al*. [25] have numerically analyzed that the output power could be increased with up to ~1% of reflectivity output coupler. Further optimization of output power with detailed reflectivity lower than 10% of output coupler needs to be experimentally investigated in our proposed DPAL, which is being pursued by the authors. In order to obtain the maximum output power, the temperature of the Cs cell was also optimized. The atomic density of Cs vapor was determined by the temperature of the Cs cell, and would severely affect the laser output power [25, 26]. If the temperature is too low, the laser oscillation is not started because of lack of gain. And if the temperature is too high, output is reduced because of reabsorption at the gain medium [27, 28]. Figure 4(b) shows the dependence of output power on the temperature of the Cs cell with 10% reflectivity output coupler. We could optimize the temperature of the Cs cell to be 130°C with maximum output power of 1.4 W using the 2.9 W of pump power. The atomic density of Cs vapor at 130°C was estimated to be 8.41×10^{13} cm^{-3} [29]. Note that these experiments were conducted with the frequency locked pump laser.

In Fig. 5(a), the blue and black lines indicate the output power as a function of pump power in the same optimized cavity when the frequency locking was applied and not applied, respectively. By applying the frequency locking, the optimized output power of 1.4 W was obtained with pump power of 2.9 W, providing the slope efficiency of 61.5% and the optical-to-optical efficiency of 49.2%. Note that when the frequency locking is not applied, the output power was decreased by ~0.1 W with the output power of 1.3 W, providing the optical-to-optical efficiency of 44.5% and the slope efficiency of 54% as shown in of Fig. 5(a). Furthermore, the fluctuation of output power in a few seconds was decreased from ~3% to ~1% by applying the frequency locking. The beam quality of the optimized output power of 1.4 W was measured along the horizontal and vertical axes in Fig. 5(b), and the inset of Fig. 5(b) shows the beam intensity distribution profile, which exhibits a Gaussian distribution [27]. The M^2 values of horizontal and vertical axes were measured to be ~1.3 and 1.4, respectively.

III. CONCLUSION

In conclusion, we proposed, for the first time to the best knowledge of the authors, a diode-pumped Cs laser with the frequency locking of pump laser. In order to maximize and stabilize the output power of the laser, the frequency of pump laser was locked at near the center of the D_2 absorption line of the Cs atom using PID feedback loop. We experimentally investigated the output power increase of ~0.1 W by applying the frequency locking of the pump laser. Furthermore, we experimentally optimized the key parameters including operation temperature and reflectivity of output coupler, and the optimized output power of 1.4 W was achieved using the pump power of 2.9 W, providing a slope efficiency of 61.5% and optical-to-optical efficiency of 49%. We believe that the proposed frequency locking method could be applied to power scaling of DPAL.

ACKNOWLEDGMENT

This work was supported by the Research Fund of High Efficiency Laser Laboratory of Agency for Defense Development of Korea (No. UD160069BD).

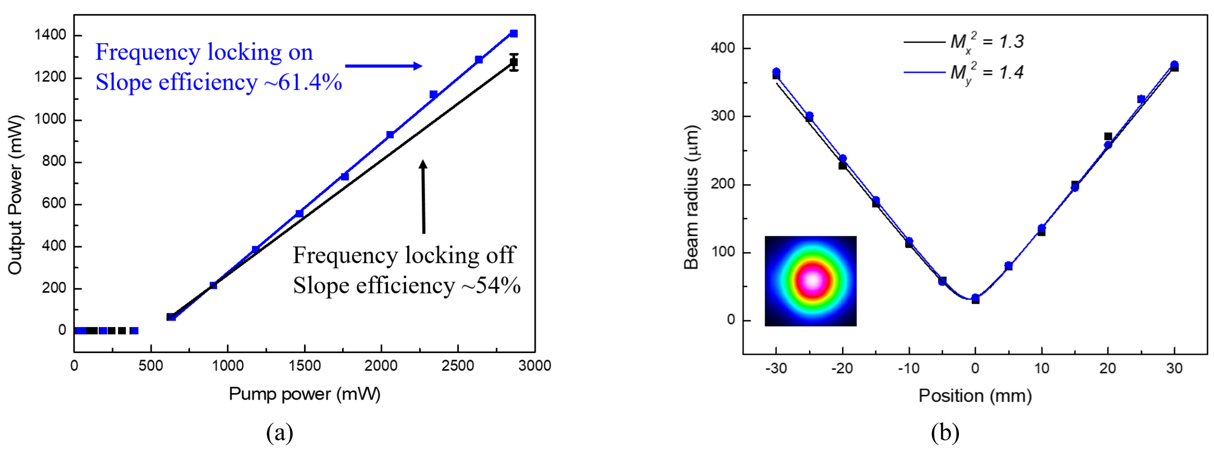

FIG. 5. (a) The output power of continuous wave laser versus incident pump power with frequency locking on and off. (b) Beam quality of output laser along the horizontal and vertical axes at the output power of 1.4 W.

REFERENCES

1. F. Gao, F. Chen, J. Xie, D. Li, L. Zhang, G. Yang, J. Guo, and L. Guo, "Review on diode-pumped alkali vapor laser," Optik - Int. J. Light Electron Opt. **124**, 4353-4358 (2013).
2. W. F. Krupke, "Diode pumped alkali lasers (DPALs)—A review (rev1)," Prog. Quant. Electron. **36**, 4-28 (2012).
3. B. Zhdanov, T. Ehrenreich, and R. Knize, "Highly efficient optically pumped cesium vapor laser," Opt. Commun. **260**, 696-698 (2006).
4. B. V. Zhdanov and R. J. Knize, "Review of alkali laser research and development," Opt. Eng. **52**, 021010 (2012).
5. J. Han, Y. Wang, H. Cai, W. Zhang, L. Xue, and H. Wang, "Algorithm for evaluation of temperature distribution of a vapor cell in a diode-pumped alkali laser system: part I," Opt. Express **22**, 13988-14003 (2014).
6. G. D. Hager and G. Perram, "A three-level analytic model for alkali metal vapor lasers: part I. Narrowband optical pumping," Appl. Phys. B **101**, 45-56 (2010).
7. M. Birnbaum, A. W. Tucker, and C. L. Fincher, "Laser emission cross section of Nd: YAG at 1064 nm," J. Appl. Phys. **52**, 1212-1215 (1981).
8. G. A. Pitz, D. E. Wertepny, and G. P. Perram, "Pressure broadening and shift of the cesium D_1 transition by the noble gases and N_2, H_2, HD, D_2, CH_4, C_2H_6, CF_4, and ^3He," Phys. Rev. A **80**, 062718 (2009).
9. H. Cai, Y. Wang, J. Han, G. An, W. Zhang, L. Xue, H. Wang, J. Zhou, M. Gao, and Z. Jiang, "Reviews of a Diode-Pumped Alkali Laser (DPAL): a potential high powered light source," in *Proc. Selected Papers from Conferences of the Photoelectronic Technology Committee of the Chinese Society of Astronautics 2014, Part I* (International Society for Optics and Photonics2015), p. 95211U.
10. W. F. Krupke, R. J. Beach, V. K. Kanz, and S. A. Payne, "DPAL: a new class of CW near-infrared high-power diode-pumped alkali (vapor) lasers," in *Proc. Gas and Chemical Lasers, and Applications III* (International Society for Optics and Photonics2004), pp. 156-168.
11. A. V. Bogachev, S. G. Garanin, A. Dudov, V. Eroshenko, S. M. Kulikov, G. Mikaelian, V. A. Panarin, V. Pautov, A. Rus, and S. A. Sukharev, "Diode-pumped caesium vapour laser with closed-cycle laser-active medium circulation," Quantum Electron. **42**, 95 (2012).
12. B. Zhdanov, G. Venus, V. Smirnov, L. Glebov, and R. Knize, "Continuous wave Cs diode pumped alkali laser pumped by single emitter narrowband laser diode," Rev. Sci. Instrum. **86**, 083104 (2015).
13. Y. Wang, M. Niigaki, H. Fukuoka, Y. Zheng, H. Miyajima, S. Matsuoka, H. Kubomura, T. Hiruma, and H. Kan, "Approaches of output improvement for a cesium vapor laser pumped by a volume-Bragg-grating coupled laser-diode-array," Phys. Lett. A **360**, 659-663 (2007).
14. B. Young, F. Cruz, W. M. Itano, and J. Bergquist, "Visible lasers with subhertz linewidths," Phys. Rev. Lett. **82**, 3799 (1999).
15. M. Bass, E. W. Van Stryland, D. R. Williams, and W. L. Wolfe, *Handbook of Optics* (McGraw-Hill New York, 1995).
16. C. E. Wieman and L. Hollberg, "Using diode lasers for atomic physics," Rev. Sci. Instrum. **62**, 1-20 (1991).
17. H. Gong, Z. Liu, Y. Zhou, and W. Zhang, "Extending the mode-hop-free tuning range of an external-cavity diode laser by synchronous tuning with mode matching," Appl. Opt. **53**, 7878-7884 (2014).
18. M. De Labachelerie and G. Passedat, "Mode-hop suppression of Littrow grating-tuned lasers," Appl. Opt. **32**, 269-274 (1993).
19. A. Liu and X. Zhang, "A review of MEMS external-cavity tunable lasers," J Micromech. Microeng. **17**, R1 (2006).
20. N. B. Jørgensen, D. Birkmose, K. Trelborg, L. Wacker, N. Winter, A. J. Hilliard, M. G. Bason, and J. J. Arlt, "A simple laser locking system based on a field-programmable gate array," Rev. Sci. Instrum. **87**, 073106 (2016).
21. J. Karlander and D. Lovric, "Frequency locking of an external cavity diode laser," Lund Reports in Atomic Physics (2011).
22. C. E. Webb and J. D. Jones, *Handbook of Laser Technology and Applications: Laser design and laser systems* (CRC Press, 2004).
23. D. A. Steck, "Cesium D line data," Los Alamos National Laboratory (unpublished) **124** (2003).
24. H. Moon, S.-E. Park, and E.-B. Kim, "Coherent multi-frequency optical source generation using a femto-second laser and its application for coherent population trapping," Opt. Express **15**, 3265-3270 (2007).
25. F. Chen, F. Gao, Y. Xu, J.-J. Xie, D.-J. Li, and J. Guo, "Study on key operating parameters of diode-pumped Cs vapor laser," in *Proc. XX International Symposium on High-Power Laser Systems and Applications 2014* (International Society for Optics and Photonics2015), p. 92551W.
26. R. J. Beach, W. F. Krupke, V. K. Kanz, S. A. Payne, M. A. Dubinskii, and L. D. Merkle, "End-pumped continuous-wave alkali vapor lasers: experiment, model, and power scaling," J. Opt. Soc. Am. B **21**, 2151-2163 (2004).
27. O. Svelto and D. C. Hanna, *Principles of lasers* (1998).
28. B. Zhdanov, A. Stooke, G. Boyadjian, A. Voci, and R. Knize, "Laser diode array pumped continuous wave Rubidium vapor laser," Opt. Express **16**, 748-751 (2008).
29. C. Alcock, V. Itkin, and M. Horrigan, "Vapour pressure equations for the metallic elements: 298-2500K," Can. Metall. Q. **23**, 309-313 (1984).